

Infrared emission from tidal disruption events — probing the pc-scale dust content around galactic nuclei

Wenbin Lu^{1*}, Pawan Kumar^{1†}, Neal J. Evans II^{1‡}

¹*Department of Astronomy, University of Texas at Austin, Austin, TX 78712, USA*

25 June 2021

ABSTRACT

Recent UV-optical surveys have been successful in finding tidal disruption events (TDEs), in which a star is tidally disrupted by a supermassive black hole (BH). These TDEs release a huge amount of radiation energy $E_{\text{rad}} \sim 10^{51} - 10^{52}$ erg into the circum-nuclear medium. If the medium is dusty, most of the radiation energy will be absorbed by dust grains within ~ 1 pc from the BH and re-radiated in the infrared. We calculate the dust emission lightcurve from a 1-D radiative transfer model, taking into account the time-dependent heating, cooling and sublimation of dust grains. We show that the dust emission peaks at $3 - 10 \mu\text{m}$ and has typical luminosities between 10^{42} and 10^{43} erg s⁻¹ (with sky covering factor of dusty clouds ranging from 0.1 to 1). This is detectable by current generation of telescopes. In the near future, *James Webb* Space Telescope will be able to perform photometric and spectroscopic measurements, in which silicate or polycyclic aromatic hydrocarbon (PAH) features may be found.

Observations at rest-frame wavelength $\geq 2 \mu\text{m}$ have only been reported from two TDE candidates, SDSS J0952+2143 and *Swift* J1644+57. Although consistent with the dust emission from TDEs, the mid-infrared fluxes of the two events may be from other sources. Long-term monitoring is needed to draw a firm conclusion. We also point out two nearby TDE candidates (ASSASN-14ae and -14li) where the dust emission may be currently detectable. The dust infrared emission can give a snapshot of the pc-scale dust content around weakly- or non-active galactic nuclei, which is hard to probe otherwise.

Key words: galaxies: nuclei — ISM: dust — infrared: ISM — methods: analytical

1 INTRODUCTION

Most galaxies harbor weakly- or non-active central supermassive black holes (BHs). Roughly once every $10^4 - 10^5$ years in each galaxy, a star enters the BH’s tidal disruption radius within which the tidal force of the BH exceeds the star’s self gravity, and hence the star gets tidally disrupted (Lacy et al. 1982; Rees 1988; Wang & Merritt 2004). In these so-called tidal disruption events (TDEs), the stellar debris feeds a burst of strong accretion that generates a bright flare of electromagnetic radiation. Several dozen such flares have been reported at various wavelengths, e.g. hard X-ray/ γ -ray (Levan et al. 2011; Bloom et al. 2011; Cenko et al. 2012), soft X-ray (reviewed by Komossa 2015), UV (e.g. Gezari et al. 2009, 2012) and optical (e.g. van Velzen et al. 2011; Arcavi et al. 2014; Vinkó et al. 2015; Holoien et al. 2015).

If a large fraction of the stellar debris is accreted by the BH, the total energy budget is $\sim \xi M_{\odot} c^2 \simeq 10^{53} \xi_{-1}$ erg, where $\xi = 0.1 \xi_{-1}$ is the efficiency of energy release from accretion and depends on the BH spin (Shakura & Sunyaev 1973). However, the observed radiation energy is usually $10^{51} - 10^{52}$ erg, much smaller than expected. Especially, the energies of the optically discovered TDEs lie at the lower end ($\sim 10^{51}$ erg). A possible solution to the “efficiency problem” could be that $\xi \ll 0.1$ because most of the stellar debris doesn’t reach the BH but is blown away by a wind at a radius of ~ 10 to 100 Schwarzschild radii (Loeb & Ulmer 1997; Ulmer 1999; Strubbe & Quataert 2009; Miller 2015; Metzger & Stone 2015; Lu & Kumar 2015). If the wind is dense enough, the effective photosphere could be far from the surface of the disk, and the radiation energy suffers from adiabatic loss before escaping, so the spectrum appears redder and the total radiation energy lower. Another possibility is that the spectral energy distribution (SED) peaks between the observable far UV and soft X-ray windows.

We can see that TDEs release a huge amount of radiation energy, which will have a significant impact on the

* wenbinlu@astro.as.utexas.edu

† pk@astro.as.utexas.edu

‡ nje@astro.as.utexas.edu

interstellar medium in the immediate vicinity of the BH. For example, as pointed out by [Ulmer \(1999\)](#), if most of the flare’s energy is radiated in the extreme UV ($\sim 10\text{--}100\text{ eV}$), the bright flash can ionize gas of mass

$$M_{\text{ion}} \simeq \frac{1.3m_{\text{H}}E_{\text{rad}}}{25\text{ eV}} \simeq 8.1 \times 10^4 M_{\odot} E_{\text{rad},51.5} \quad (1)$$

out to a radius

$$R_{\text{ion}} \simeq \left(\frac{3}{4\pi n_{\text{H}}} \frac{E_{\text{rad}}}{25\text{ eV}} \right)^{1/3} \simeq 2.6 \times 10^{19} \left(\frac{E_{\text{rad},51.5}}{n_{\text{H},3}} \right)^{1/3} \text{ cm} \quad (2)$$

where $E_{\text{rad}} = 3 \times 10^{51} E_{\text{rad},51.5}$ erg, $n_{\text{H}} = 10^3 n_{\text{H},3} \text{ cm}^{-3}$ is the number density of H nuclei and we have assumed each H nucleus consumes 25 eV (ionization potential of H and He + bond energy of H_2 + kinetic energy of free protons and electrons). In eq.(1) and (2), recombination is ignored because the timescale $t_{\text{rec}} \sim 10^3 n_{\text{H},3}^{-1} T_4^{1/2}$ yr is expected to be long. Then the energy of the ionizing flash will be slowly reprocessed into potentially observable H and He recombination lines if the gas density is high, or forbidden lines (of metals) if the gas density is low.

However, eq.(1) and (2) are true only if there is no dust extinction. If dust is well mixed with the gas, the V-band extinction is proportional to the gas column density and we have $A_{\text{V}}/N_{\text{H}} \simeq 5.3 \times 10^{-22} \text{ mag cm}^2 \text{ H}^{-1}$ for sightlines with $R_{\text{V}} \equiv A_{\text{V}}/E(B-V) = 3.1$ ([Draine 2011](#)). The V-band extinction of the gas with a column depth of $N_{\text{H}} = n_{\text{H}} R_{\text{ion}} = 2.6 \times 10^{22} n_{\text{H},3}^{2/3} E_{\text{rad},51.5}^{1/3}$ is

$$A_{\text{V}} \simeq 14 n_{\text{H},3}^{2/3} E_{\text{rad},51.5}^{1/3} \text{ mag} \quad (3)$$

Therefore, for our fiducial galactic center density of $n_{\text{H}} = 10^3 \text{ cm}^{-3}$, the ionizing flash will be significantly attenuated at a radius of $\sim 2 \times 10^{18} \text{ cm}$, unless dust is significantly depleted in the gas before the TDE occurs.

The radiation energy will be deposited into dust grains, which then re-radiate in the infrared (IR). A similar process has been studied in the context of gamma-ray bursts (GRBs) by [Waxman & Draine \(2000\)](#) and [Draine & Hao \(2002\)](#). As we show in this work, if a significant amount of dust exists in the pc-scale vicinity of the BH, the dust IR emission from TDEs is much brighter than that from GRBs, lasts longer, and is hence easier to observe.

Before moving forward to calculations of the dust IR emission, we summarize our current (very limited) knowledge about the pc-scale dust content around galactic nuclei.

In the context of active galactic nuclei (AGN), the accretion disk and broad line region are surrounded by a thick dusty torus (e.g. [Jaffe et al. 2004](#); [Tristram et al. 2007](#); [Elitzur 2008](#)). The dusty torus absorbs a significant fraction of nuclear luminosity and re-radiates mid-IR continuum as observed in most AGNs. Typically, the sky covering factor of the torus is $\sim 1/2$ and inner boundary is roughly given by the dust sublimation radius $\sim 0.4 L_{45}^{1/2}$ pc, where $L = 10^{45} L_{45} \text{ erg s}^{-1}$ is the disk luminosity ([Nenkova et al. 2008](#)). The torus is dynamically active ([Krolik & Begelman 1988](#)), possibly coming from a clumpy wind launched from the accretion disk ([Emmering et al. 1992](#); [Konigl & Kartje 1994](#)). For weakly-active galactic nuclei with luminosities $L \lesssim 10^{42} \text{ erg s}^{-1}$, the accretion disk can no longer sustain a wind outflow rate required by the mid-IR emission extrapolated from high-luminosity AGNs, so the torus

is expected to disappear ([Elitzur & Shlosman 2006](#)). This has not been observationally confirmed, because the dust emission no longer dominates in the mid-IR when $L \lesssim 10^{42} \text{ erg s}^{-1}$ ([González-Martín et al. 2015](#)). As pointed out by [Elitzur & Shlosman \(2006\)](#), even at these luminosities, the disk outflow can still provide a small but significant toroidal obscuration as long as the column density exceeds $\sim 10^{21} \text{ cm}^{-2}$.

In the context of non-active galactic nuclei, the nuclear dust content is hard to probe due to the overwhelming starlight and telescopes’ limited angular resolution (1 arcsec $\sim 50 \text{ pc}$ at a distance of 10 Mpc). Currently, the only observable case is our Galactic Center. Radio observations (of tracer molecules) revealed $\sim 10^5 M_{\odot}$ of molecular clouds and diffuse molecular gas at $\sim 1\text{--}5 \text{ pc}$ from the BH, mostly in a torus-like structure (known as circum-nuclear disk, CND) with a sky covering factor $\sim 30\%$ viewed from the BH (e.g. [Herrnstein & Ho 2005](#); [Christopher et al. 2005](#); [Ferrière 2012](#)). Inward from the CND, due to the radiation from the central star cluster ($\sim 10^7 L_{\odot}$), the gas becomes atomic and then ionized. The photo-dissociation region and HII region are both dusty and are observable through atomic fine-structure lines ([Serabyn & Lacy 1985](#); [Jackson et al. 1993](#)), free-free continuum ([Roberts & Goss 1993](#)), recombination lines ([Scoville et al. 2003](#)), and mid/far-IR dust thermal emission ([Lau et al. 2013](#)). The densities of different regions estimated by these works are $n_{\text{H}} \sim 10^3 \text{ cm}^{-3}$ (HII regions), 10^4 cm^{-3} (warm neutral medium and molecular streamers), and 10^5 cm^{-3} (molecular cores).

The dust within a few parsecs of the Galactic Center may originate from infalling molecular clouds/clumps ([Jackson et al. 1993](#)) or from *in-situ* dust formation ([Lau et al. 2015](#)). Dust grains may be destroyed by two processes: sublimation and sputtering. The former may be unimportant because the dust sublimation radius is $\ll 1 \text{ pc}$ in weakly- or non-active galactic nuclei. The latter process is significant only in the shock heated hot ionized medium where the gas temperature $\gtrsim 10^{5.5} \text{ K}$.

We note the fact that the Galactic Center is unusually dusty may be because the Milky Way is a gas-rich star-forming galaxy. The nuclear dust content of elliptical galaxies is unknown but may be much less than in our Galaxy. As we show in this work, the pc-scale dust content around galactic nuclei can be probed by searching for the dust IR emission after a TDE is discovered. In section 2, we give an order-of-magnitude estimation of the IR emission from the dust heated by TDEs. In section 3, we calculate the bolometric lightcurve from a 1-D time-dependent radiative transfer model. In section 4, we discuss the detectability and implications, as well as some possible issues in our simple calculations. A short summary is given in section 5.

2 ORDER-OF-MAGNITUDE ESTIMATION

Lacking the knowledge of the dust distribution, we assume spherical symmetry for simplicity. Consider a point source with UV-optical luminosity $L(t)$ as a function of time t in the rest frame of the source. We assume a uniform spatial distribution of dust grains with number density n_{d} , spanning from inner radius R_{in} to outer radius R_{out} . As the UV-optical radiation propagates through the cloud, dust grains

will be heated up. For a grain of radius a at radius R from the source, its temperature T is determined by the equilibrium between heating and radiative plus grain-sublimation cooling (Waxman & Draine 2000)

$$e^{-\tau_{UV}} \frac{L(t_r)}{4\pi R^2} \pi a^2 Q_{UV} = \langle Q_{abs} \rangle_P 4\pi a^2 \sigma T^4 - 4\pi a^2 \frac{da}{dt} \frac{\rho}{\mu} B \quad (4)$$

where $e^{-\tau_{UV}}$ is the effective attenuation of the UV-optical flash by inner dust shells, $t_r = t - R/c$ is the “retarded” time (corresponding to the time segment of the UV-optical flash), $Q_{UV} \simeq 1$ (Draine 2011) is the absorption efficiency factor of UV-optical radiation,

$$\langle Q_{abs} \rangle_P \equiv \frac{\int B_\nu(T) Q_{abs}(\nu) d\nu}{\int B_\nu(T) d\nu} \quad (5)$$

is the Planck-averaged absorption efficiency factor, σ is the Stefan-Boltzmann constant, ρ is the density of the grain material, μ is the mean atomic mass, and B is the chemical binding energy. For the temperature range of interest in this work $1000 \lesssim T \lesssim 2500$ K, we use an intermediate absorption coefficient between astronomical silicate and graphite (Waxman & Draine 2000)

$$\langle Q_{abs} \rangle_P \simeq \frac{0.1 a_{-5} (T/2300 \text{ K})}{1 + 0.1 a_{-5} (T/2300 \text{ K})} \quad (6)$$

where the grain radius is normalized to a typical value of $a = 10^{-5} a_{-5}$ cm. The thermal sublimation rate is a function of temperature and can be estimated by

$$\frac{da}{dt} = -\nu_0 \left(\frac{\mu}{\rho} \right)^{1/3} e^{-B/kT} \quad (7)$$

We take $\nu_0 \simeq 1 \times 10^{15} \text{ s}^{-1}$, $B/k = 7 \times 10^4$ K, and $\rho/\mu = 1 \times 10^{23} \text{ cm}^{-3}$ as representative values for refractory grains (Guhathakurta & Draine 1989; Waxman & Draine 2000). From eq.(7), we get a characteristic grain survival time at temperature T

$$t_{\text{surv}}(T) = \frac{a}{|da/dt|} = 4.9 \times 10^6 a_{-5} \cdot \exp \left[7 \times 10^4 \text{ K} \left(\frac{1}{T} - \frac{1}{1600 \text{ K}} \right) \right] \text{ s} \quad (8)$$

If the duration of the TDE UV-optical flash is $t_{\text{TDE}} = 10^6 t_{\text{TDE},6}$ s, the “sublimation temperature” (above which dust grains fully sublime) can be defined by $t_{\text{surv}}(T_{\text{sub}}) = t_{\text{TDE}}$, i.e.

$$T_{\text{sub}} = 1.66 \times 10^3 \left[1 + 2.37 \times 10^{-2} \ln \frac{t_{\text{TDE},6}}{a_{-5}} \right] \text{ K} \quad (9)$$

It can be shown that the critical temperature at which radiative cooling equals to sublimation cooling is $T_{r=s} \simeq 2800$ K, so the sublimation cooling term in eq.(4) is usually negligible and we can solve for the “sublimation radius” where the grain temperature equals to T_{sub}

$$R_{\text{sub}} = 1.4 \times 10^{18} \left[L_{45.5} e^{-\tau_{UV}} a_{-5}^{-1} (1 + 0.072 a_{-5}) \right]^{1/2} \text{ cm} \quad (10)$$

If the whole dusty layer is optically thick to the UV-optical radiation from the central source, the total radiation energy $E_{\text{rad}} = 3 \times 10^{51} E_{\text{rad},51.5}$ erg will be absorbed and re-radiated at a typical wavelength of $\lambda \simeq 3(T/1600 \text{ K})^{-1} \mu\text{m}$. Because the dust sublimation rate increases steeply with grain temperature (eq. 7), grains at radii $R < R_{\text{sub}}$ sublime fully before a significant fraction of UV-optical energy is absorbed.

From eq.(9), we can see that dust IR emission usually cuts off at wavelength shorter than $3 \mu\text{m}$, unless there is more dust at $R < R_{\text{sub}}$ than the UV-optical radiation can cause to sublime. The duration of the dust emission can be estimated by the light-crossing time $2R_{\text{sub}}/c \simeq 6.5 R_{\text{sub},\text{pc}} \text{ yr}$, where c is the speed of light and $R_{\text{sub},\text{pc}} = R_{\text{sub}}/1 \text{ pc}$. The IR luminosity of the dust emission can be estimated by

$$L_{\text{IR}} \simeq \frac{E_{\text{rad}} f_\Omega}{2R_{\text{sub}}/c} e^{-\tau_{\text{IR}}} \simeq 1.5 \times 10^{43} \frac{E_{\text{rad},51.5}}{R_{\text{sub},\text{pc}}} f_\Omega e^{-\tau_{\text{IR}}} \text{ erg/s} \quad (11)$$

where f_Ω is the sky covering factor of the dusty clouds viewed from the BH and $e^{-\tau_{\text{IR}}}$ is the further attenuation of the dust IR emission by outer dust shells that are not heated up. Note that, when the dusty cloud is far enough from the central source that sublimation is not significant, most IR emission comes from the inner edge of the cloud and R_{sub} should be replaced by R_{in} . Also, eq.(11) is a conservative estimate because when $f_\Omega < 1$, say the plane of the dust torus is oriented at an angle θ wrt. the line of sight, the light-crossing time is a factor of $\cos \theta$ shorter than $2R_{\text{sub}}/c$.

3 RADIATIVE TRANSFER

In this section, we model the heating and cooling of dust grains with time-dependent radiative transfer in a 1-D spherical symmetric grid. The bolometric lightcurve of dust IR emission is calculated.

3.1 Model description

Dust is distributed uniformly in the spherical layer between the inner radius R_{in} and outer radius R_{out} . We assume all dust grains have the same initial radius a_0 and the number density n_d is independent of radius. We divide the whole dust layer into N thin shells of thickness ΔR and the middle point radius of the j -th shell ($j = 1, 2, 3, \dots, N$) is R_j . Due to sublimation, the grain radius in the j -th shell $a_j(t_r)$ is a function of the retarded time t_r (local time since the arrival of the radiation front). The total optical depth from R_{in} to R_j is

$$\tau_j = \sum_{i=0}^{j-1} \Delta \tau_i = \sum_{i=0}^{j-1} (\pi a_i^2 n_d Q_{UV,\text{ext}} \Delta R) \quad (12)$$

where the extinction coefficient factor $Q_{UV,\text{ext}} = 2$ is from nearly equal contributions from absorption and scattering at UV-optical wavelengths (Draine 2011). Note that the photons with scattering angle θ_s , after traveling a distance δR , are delayed by

$$\delta t = \frac{\delta R (1 - \cos \theta_s)}{c} = 10^6 \frac{\delta R}{10^{17} \text{ cm}} \frac{1 - \cos \theta_s}{0.3} \text{ s}, \quad (13)$$

so the scattered photons suffer from significant delays. To keep the model simple and conservative, we ignore the absorption of the scattered photons. We also ignore the small contribution to dust heating by the IR radiation from other shells, because of the time delay and the extinction at IR wavelength being small. For instance, $A_{3\mu\text{m}}/A_V = 0.069$ for $R_V = 3.1$ (Cardelli et al. 1989). Actually, the heating flux on dust grains from UV and IR photons bouncing between different layers is a factor of $\sim 10^2$ smaller than the flux

directly from the central source ($\sim E_{\text{rad}}c/8\pi R^3$ instead of $L/4\pi R^2$ on the left hand side of eq. 4). Therefore, on the light-crossing timescale (a few years), the grain temperature is a factor of ~ 3 smaller and hence the reprocessed emission is around $10 \mu\text{m}$.

Combining eq.(4), (5) and (7), we use a simple explicit scheme to solve the time evolution of grain temperatures $T_j(t_r)$ and radii $a_j(t_r)$ in each shell. We take the time step to be one tenth of the local grain survival time

$$\Delta t = t_{\text{surv}}(R)/10 \quad (14)$$

We have tested that the results are not affected by a factor of 2 variations in Δt in all cases presented. As shown below, if we only consider the dusty region to be at radius $R \gtrsim 0.3 \text{ pc}$, the grain temperatures are always smaller than $T_{r=s}$ (the temperature at which the radiative cooling equals to sublimation cooling). Since the sublimation cooling term in eq.(4) drops fast with decreasing temperature [$\propto \exp(-7 \times 10^4 K/T)$], we ignore the sublimation cooling term in our calculations.

From $\{T_j(t_r), a_j(t_r)\}$, we get the volume emissivity ($\text{erg cm}^{-3} \text{ s}^{-1} \text{ sr}^{-1}$) of the j -th shell

$$J_{\text{IR},j}(t_r) = 4\pi a_j^2 n_d \langle Q_{\text{abs}} \rangle_P \sigma T_j^4 / 4\pi \quad (15)$$

as a function of retarded time through $T_j(t_r)$ and $a_j(t_r)$. At any observer's time t_{obs} , we can add up the contributions from all the shells at different radii R and emission latitudes θ to get the total (isotropic equivalent) IR luminosity

$$L_{\text{IR}}(t_{\text{obs}}) = 4\pi \int_{R_{\text{in}}}^{R_{\text{out}}} R^2 dR \int_0^\pi 2\pi \sin \theta d\theta \cdot J_{\text{IR}}(R, \theta, t_r) e^{-\tau_{\text{IR}}(R, \theta, t_r)} \quad (16)$$

where $e^{-\tau_{\text{IR}}}$ is the attenuation of the IR emission from position (R, θ) at t_r by other dust shells along the line of sight. The observer's clock starts ($t_{\text{obs}} = 0$) when the radiation front from the central source arrives, so the IR photons emitted from position (R, θ) at retarded time t_r will reach the observer at

$$t_{\text{obs}} = R(1 - \cos \theta)/c + t_r \quad (17)$$

which gives t_r as a function of t_{obs} , R and θ .

To calculate the IR optical depth $\tau_{\text{IR}}(R, \theta, t_r)$, we integrate the absorption¹ by dust shells along the line of sight. As shown in Fig.(1), there are two cases: (1) if the emission latitude $\theta < 90^\circ$, the line of sight intersects once with all the outer shells ($R_{\text{ab}} > R$); (2) if the $\theta > 90^\circ$, the line of sight intersects once with all the outer shells and twice with the inner shells at radii $R \sin \theta < R_{\text{ab}} < R$. We denote the angle between the light ray and radial direction as θ_{ab} and it satisfies

$$\sin \theta_{\text{ab}} = \frac{R \sin \theta}{R_{\text{ab}}} \quad (18)$$

To calculate the optical depth contributed by each shell, we

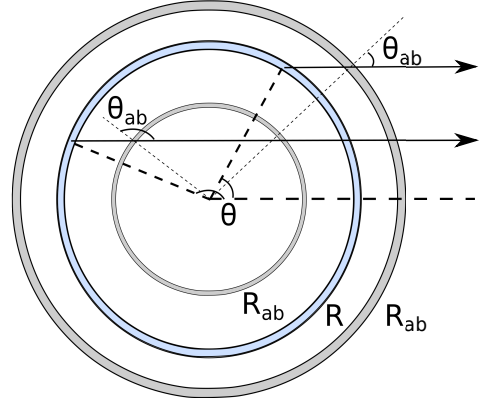


Figure 1. The geometry of the extinction of the dust IR emission by the other shells along the line of sight. The observer is at infinity on the right-hand side. The IR light rays from the shell at radius R may intersect with inner or outer absorbing shells, whose radii are denoted as R_{ab} . There are two possible cases: (1) if the emission latitude $\theta < 90^\circ$, the line of sight intersects once with all the outer shells ($R_{\text{ab}} > R$); (2) if $\theta > 90^\circ$, the line of sight intersects once with all the outer shells and twice with the inner shells at radii $R \sin \theta < R_{\text{ab}} < R$.

need to know the dust content at the shell's retarded time when the IR light ray arrives

$$t_{r,\text{ab}} = \begin{cases} t_r + [R(1 - \cos \theta)]/c, & \text{if } R_{\text{ab}} > R \\ t_r + [-R \cos \theta + R_{\text{ab}} \cos \theta_{\text{ab}}]/c, & \text{if } R_{\text{ab}} < R \end{cases} \quad (19)$$

Note that when the IR light ray arrives at an inner shell for the first time, we have $\theta_{\text{ab}} > 90^\circ$ and hence $\cos \theta_{\text{ab}} < 0$. In the model, the grain number density n_d is fixed and the decreasing of dust content in a shell (due to sublimation) is captured by the decreasing of grain radii with its retarded time $a(t_r)$. When $a(t_r)$ is smaller than $1/30$ of the initial grain radius a_0 , we consider the grain sublimation to be complete and the shell becomes dust free. Therefore, we can calculate the optical depth of the IR emission from position (R, θ) at t_r : (1) the contribution from outer shells

$$\tau_{\text{IR}}^{\text{out}}(R, \theta, t_r) = \int_R^{R_{\text{out}}} \frac{dR_{\text{ab}}}{|\cos \theta_{\text{ab}}|} n_d \pi a^2 \langle Q_{\text{abs}} \rangle_P \quad (20)$$

(2) the contribution from inner shells (only when $\theta > 90^\circ$)

$$\tau_{\text{IR}}^{\text{in}}(R, \theta, t_r) = \int_{R \sin \theta}^R \frac{dR_{\text{ab}}}{|\cos \theta_{\text{ab}}|} n_d \sum_{i=1,2} \left(\pi a_i^2 \langle Q_{\text{abs}} \rangle_{P,i} \right) \quad (21)$$

where $i = 1, 2$ means the first/second time the IR light ray intersects with the absorbing shell. Note that the Planck-averaged absorption efficiency factor $\langle Q_{\text{abs}} \rangle_P$ (eq. 6) depends on the grain size a in the absorbing shell (at R_{ab} , $t_{r,\text{ab}}$) and the radiation temperature² T of the emitting shell (at R , t_r).

¹ Since the grain sizes are smaller than the typical dust emission wavelength ($\lambda \gtrsim 3 \mu\text{m}$), scattering has a smaller cross section than absorption, so we ignore the contribution to the IR optical depth from scattering.

² The spectrum of dust emission from a thin shell at temperature T is assumed to be Planckian. We note that, as the IR light ray propagates through the dust shells, the spectrum will change due to reddening. However, in all computed cases, the absorption at IR wavelength ($\lambda \gtrsim 3 \mu\text{m}$) is not very large, so the changing of spectrum is ignored.

Table 1. Summary of the four cases, where we vary the inner edge of the dusty cloud R_{in} , the UV-optical luminosity L_0 and duration t_{TDE} of the TDE source. The lightcurve of the source is assumed to be flat. The following parameters are fixed in all four cases: the radial thickness of the dusty cloud $R_{\text{out}} - R_{\text{in}} = 1$ pc, initial grain radius $a_0 = 0.1 \mu\text{m}$ (all grains having the same initial radius) and the total dust optical depth $\tau_{UV} = 10$ ($A_V \simeq 10$ mag).

Case No.	R_{in} [pc]	L_0 [erg/s]	t_{TDE} [s]
I	0.3	3×10^{45}	10^6
II	1	3×10^{45}	10^6
III	1	1×10^{46}	10^6
IV	1	3×10^{44}	10^7

3.2 Results

We run the 1-D radiative transfer model for four cases, which are summarized in Table 1. The following parameters are fixed in all four cases: the radial thickness of the dusty cloud $R_{\text{out}} - R_{\text{in}} = 1$ pc, initial grain radius $a_0 = 0.1 \mu\text{m}$ (all grains having the same initial radius) and the total dust optical depth $\tau_{UV} = 10$ ($A_V \simeq 10$ mag). The grain number density is constant with radius and is given by³

$$n_d = \frac{\tau_{UV}}{Q_{UV, \text{ext}} \pi a_0^2 (R_{\text{out}} - R_{\text{in}})} \simeq 5.1 \times 10^{-9} \text{ cm}^{-3} \quad (22)$$

where the extinction coefficient factor $Q_{UV, \text{ext}} = 2$ (equal contributions from absorption and scattering).

The bolometric lightcurves for all cases are shown in Fig.(2), from which we draw the following conclusions: (1) the luminosities are determined by the total energy input E_{rad} and the light-travel delay, and are typically $\sim 10^{43} \text{ erg s}^{-1}$, consistent with the estimation in eq.(11); (2) the lightcurves rise linearly until t_{TDE} (due to the increasing emitting area) and when $t_{\text{obs}} \gg t_{\text{TDE}}$, the lightcurves are nearly flat⁴. To illustrate the dust sublimation process, in Fig.(3) we show the grain temperature and radius profiles for case I (red curve in Fig. 2) at different retarded time $t_r = 3 \times 10^4, 3 \times 10^5, 1 \times 10^6$ s. We can see that the dust sublimation front is very sharp and moves outwards with time. At $t_r = t_{\text{TDE}} = 1 \times 10^6$ s, the dust grains in the inner quarter (radius-wise) of the cloud have fully sublimated. In case I, the IR emission peaks at $\sim 3 \mu\text{m}$. The temperature profile far beyond the sublimation front is exponential, as expected from the $e^{-\tau_{UV}}$ term in eq.(4). We note that, at larger radii where the temperature drops to much below 1000 K, the absorption coefficient adopted in eq.(6) may not be a good approximation. However, since most IR emission comes from the inner-most shells where the grain temperatures are high, our results are not affected.

³ If the density of the grain material is $\rho = 2 \text{ g cm}^{-3}$, the grain number density n_d corresponds to mass density of $4.3 \times 10^{-23} \text{ g cm}^{-3}$. Using a dust-to-gas mass ratio of 0.01, we get a hydrogen number density of $n_H \simeq 3 \times 10^3 \text{ cm}^{-3}$.

⁴ The small dip in each lightcurve towards the end corresponds to the emission from altitude angle $\theta \simeq 90^\circ$ (where the projected surface area is slightly smaller).

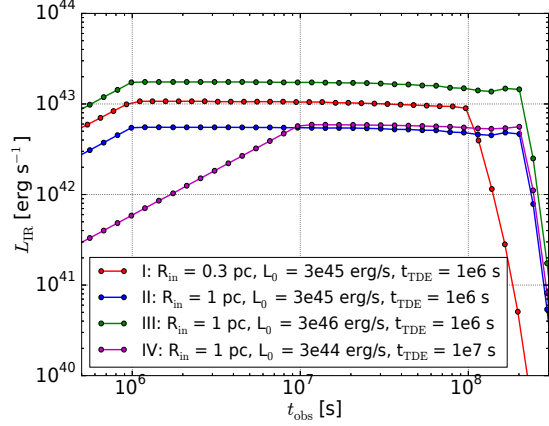


Figure 2. Bolometric lightcurves of dust IR emission from the 1-D time-dependent radiative transfer model. The dust IR emission lasts for a few years with a typical luminosity of $\sim 10^{43} \text{ erg s}^{-1}$, consistent with the estimation in eq.(11). The legend shows the variable parameters in each case and the fixed common parameters are described in the caption of Table 1.

4 DISCUSSION

4.1 Detectability

As shown in section 2 and 3, for $f_\Omega \sim 0.1 - 1$ (the fraction of UV-optical radiation from the TDE intercepted by dust in the central few parsecs), the dust IR emission has a typical bolometric luminosity of $L_{\text{bol}} \sim 10^{42} - 10^{43} \text{ erg s}^{-1}$ and peaks at $\nu_{\text{peak}} \simeq 9.4 \times 10^{13} (T/1600 \text{ K}) \text{ Hz}$ ($\sim 3 \mu\text{m}$). For a luminosity distance of $d_L = 1 \text{ Gpc}$ (redshift $z \simeq 0.2$), the peak flux density is $F_{\nu, \text{peak}} \simeq L_{\text{bol}} / (4\pi d_L^2 \nu_{\text{peak}}) \simeq 0.01 - 0.1 \text{ mJy}$. This is photometrically detectable by current generation of telescopes, including the Stratospheric Observatory for Infrared Astronomy⁵ (SOFIA, with the FLITECAM and FORCAST instruments) and the *Spitzer* Space Telescope⁶ (hereafter *Spitzer*, with the IRAC instrument). In the near future, *James Webb* Space Telescope⁷ (JWST) will be able to perform photometric and spectroscopic measurements.

We note that ground-based telescopes are much more sensitive at $2 \mu\text{m}$ (K band) than at $\gtrsim 3 \mu\text{m}$. Observations at $\gtrsim 3 \mu\text{m}$ by space telescopes are more useful at detecting dust IR emission due to the following two reasons: (1) at wavelengths close to the optical, the flux could be dominated by other bright sources such as the accretion disk (as shown in Fig. 5 below) or star light; (2) since the extinction ratio $A_{2\mu\text{m}}/A_{3\mu\text{m}} \simeq 2$ (Cardelli et al. 1989), dust emission at $\lesssim 2 \mu\text{m}$ may be significantly absorbed by outer dusty layers (and re-radiated at longer wavelengths). However, on one hand, the confusion by the disk emission could be ruled out by long-term monitoring, since the disk accretion rate is expected to drop fast with time while the luminosity from dust emission stays more-or-less constant for many years. On the other hand, a combination of high UV-optical luminosities (L_0) and small inner edge radii (R_{in}) can lead to relatively

⁵ <https://www.sofia.usra.edu/>

⁶ <http://www.spitzer.caltech.edu/>

⁷ <http://www.stsci.edu/jwst/science/sensitivity>

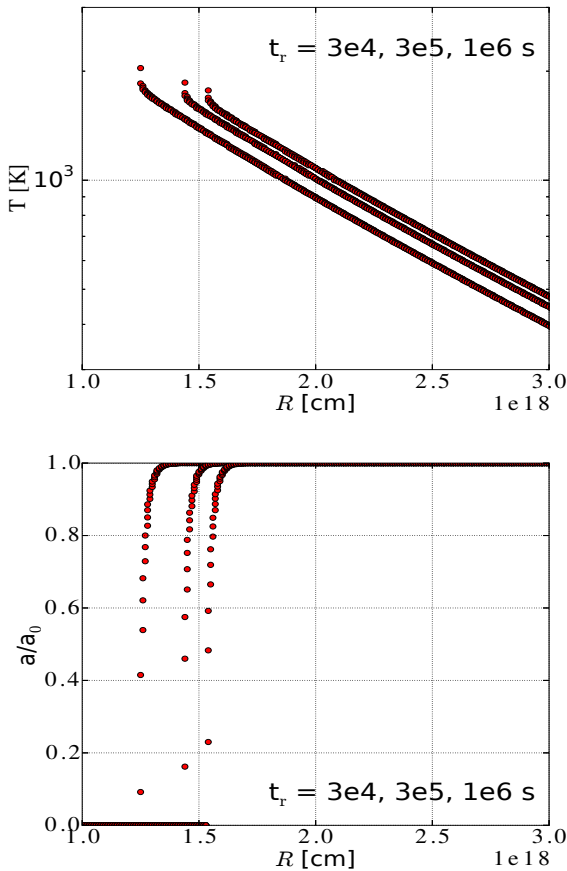


Figure 3. The upper and low panels are respectively the grain temperature and radius profiles for case I (red curve in Fig. 2) at different retarded time $t_r = 3 \times 10^4, 3 \times 10^5, 1 \times 10^6$ s. We can see that the dust sublimation front is very sharp and moves outwards with time. The temperature profile far beyond the sublimation front is exponential, as expected from the $e^{-\tau_{UV}}$ term in eq.(4). When $a(t_r) < a_0/30$, we consider the grain sublimation to be complete and set $a(t_r) = 0$. This is the reason for the radius “floor” at small radii.

high grain temperatures, such as in case I (red curve in Fig. 2). For example, the flux density ratio $F_{2\mu\text{m}}/F_{3\mu\text{m}}$ of a black-body at $T = 1600$ K is only 0.72, so ground-based K-band observations may play an important role in studying dust IR emission.

To the authors’ knowledge, IR observations at rest-frame wavelength $\geq 2 \mu\text{m}$ have only been reported from two TDE candidates, SDSS J0952+2143 (Komossa et al. 2008, 2009) and *Swift* J1644+57 (Yoon et al. 2015; Levan et al. 2015). Below, we first show that the mid-IR flux from SDSS J0952+2143, although consistent with the dust emission from a TDE, is likely permanent emission from dust-obscured starburst regions or an AGN. Then, we also show that the mid-IR flux from *Swift* J1644+57 may be produced by other radiation sources, such as the accretion disk or the external shock driven by the interaction between disk outflow and circum-nuclear medium. Therefore, we are not sure whether the dust IR emission calculated in this work has been detected. At last, we point out two TDE candidates where the dust IR emission may be currently detectable.

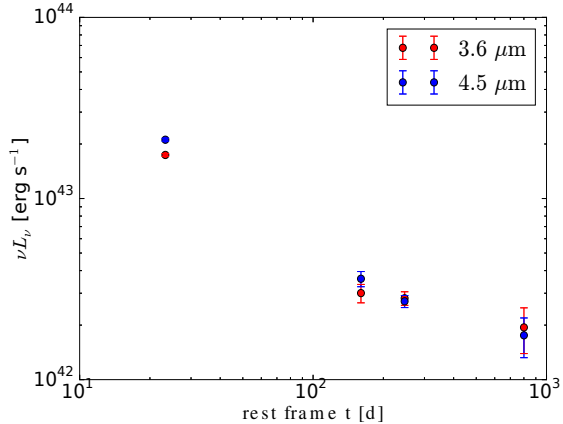


Figure 4. Lightcurves of *Swift* J1644+57 at the *Spitzer* 3.6 μm and 4.5 μm bands. The flux from the host galaxy is included and the extinction is not corrected. The data comes from Yoon et al. (2015); Levan et al. (2015).

SDSS J0952+2143 (redshift $z = 0.079$) was reported as a TDE candidate due to its strong but transient emission lines (of e.g. H, He, Fe), which are interpreted as the light echo of a powerful EUV-X-ray outburst (not directly observed). Photometry from Sloan Digital Sky Survey showed a fading optical continuum since Dec 2004 and the outburst is believed to have happened before this time. Near-IR (J, H and K_s -band) images showed quiescent (from 1998 to 2008) emission of $L_{\text{NIR}} \simeq 2.5 \times 10^{43} \text{ erg s}^{-1}$ dominated by the extended host galaxy. A *Spitzer* mid-IR (10–20 μm) spectrum obtained in Jun 2008 showed two pronounced silicate peaks at ~ 10 and $\sim 18 \mu\text{m}$, which resemble the SEDs of many Palomar-Green quasars (Netzer et al. 2007). The integrated luminosity was $L_{10-20\mu\text{m}} = 3.5 \times 10^{43} \text{ erg s}^{-1}$. The total amount of energy radiated in the observation window since the outburst is $\sim 3.5 \times 10^{51} \text{ erg}$ and the grain temperature can be estimated to be $\sim 300 - 500$ K. Therefore, the mid-IR data is consistent with the scenario of emission from the circum-nuclear dust heated by a TDE. However, as pointed out by Komossa et al. (2009), the whole SED from optical to mid-IR could also be produced by dusty starburst regions. In addition, an X-ray luminosity of $10^{41} \text{ erg s}^{-1}$ may be due to a weak AGN, which could also contribute some mid-IR flux. Another mid-IR observation is needed to tell whether the mid-IR emission is transient or permanent.

Swift J1644+57 (redshift $z = 0.35$) is widely believed to be a special TDE where a relativistic outflow is launched from the accretion disk and produces bright emission from γ -ray to radio wavelengths (e.g. Levan et al. 2011; Bloom et al. 2011; Zauderer et al. 2011). This event received excellent observational coverages in the time domain (a few to ~ 1000 days) and wavelength domain ($\sim \text{GHz}$ to $\sim \text{TeV}$). Due to heavy host extinction ($A_V \sim 10 \text{ mag}$), the UV and optical fluxes are strongly suppressed. For the purpose of this work, we pay attention to the *Spitzer* 3.6 μm (rest-frame $\nu = 1.1 \times 10^{14} \text{ Hz}$) and 4.5 μm (rest-frame $\nu = 9.0 \times 10^{13} \text{ Hz}$) data and see if it originates from the dust IR emission.

In Fig.(4), we plot the 3.6 μm and 4.5 μm band lightcurves, with the flux from the host galaxy included and the host extinction is not corrected. The latest data points

(at rest-frame $t \sim 800$ d) are considered as host flux, although the lightcurves are not completely flat. In a similar way, the host flux in J, H, and K bands are obtained and reported by [Levan et al. \(2015\)](#). In Fig.(5), we plot the SEDs with the radio data from [Zauderer et al. \(2013\)](#) and the host-subtracted IR data from [Yoon et al. \(2015\)](#); [Levan et al. \(2015\)](#) at rest-frame time $t \simeq 150$ d and 250 d.

On the high-frequency side, the $3.6 \mu\text{m}$ and $4.5 \mu\text{m}$ fluxes are consistent with being the Rayleigh-Jeans tail of a blackbody component (especially in the lower panel at rest-frame $t \simeq 250$ d). As pointed out by [Levan et al. \(2015\)](#), the blackbody component may originate from the accretion disk.

On the low-frequency side, the radio emission has been extensively studied and is well explained by the external shock produced by the interaction between the disk outflow and circum-nuclear medium ([Metzger et al. 2012](#); [Barniol Duran & Piran 2013](#); [Zauderer et al. 2013](#); [Kumar et al. 2013](#); [Mimica et al. 2015](#)). The details of the outflow are different in different models, but at $\gtrsim 200$ days, the blast wave should more or less settle to the Sedov-Taylor evolution. In the standard external shock model (see e.g. [Kumar & Zhang 2015](#)), electrons are accelerated to a relativistic powerlaw distribution and then produce a broken powerlaw spectrum via synchrotron radiation. From Fig.(5), we can see that, if there is no spectral break between the radio and IR, the $3.6 \mu\text{m}$ and $4.5 \mu\text{m}$ fluxes are consistent with the extrapolation of the powerlaw around 10^{11} Hz. For an electron energy distribution of $dN/d\gamma_e \propto \gamma_e^{-p}$, a spectral break may be produced at the synchrotron cooling frequency ν_c , because $\nu F_\nu \propto \nu^{(1-p)/2}$ when $\nu < \nu_c$ and $\nu F_\nu \propto \nu^{1-p/2}$ when $\nu > \nu_c$. If the blast wave is sub-relativistic, the synchrotron cooling frequency is given by

$$\nu_c = \frac{27\pi q m_e c}{\sigma_T^2 B^3 t^2} \simeq 8.4 \times 10^{15} \left(\frac{B}{10 \text{ mG}} \right)^{-3} \left(\frac{t}{200 \text{ d}} \right)^{-2} \text{ Hz} \quad (23)$$

where m_e is electron mass, q is electron charge, σ_T is Thomson scattering cross-section, B is the strength of magnetic field, t is the dynamical time. From eq.(23), we can see that, as long as $B \lesssim 50$ mG, the synchrotron cooling break is expected to be above 10^{14} Hz, and hence the $3.6 \mu\text{m}$ and $4.5 \mu\text{m}$ fluxes are consistent with being produced by the external shock. The magnetic field energy density in the shocked region is usually assumed to be a fraction ϵ_B of the thermal energy density and hence depends on the circum-nuclear medium density and ϵ_B . These two parameters are very uncertain, so a firm conclusion cannot be drawn.

On the other hand, since the dust IR emission typically lasts for a few years, we encourage observations at $3 - 10 \mu\text{m}$ on some recently-discovered TDE candidates, especially the most nearby ones ASSASN-14ae ([Holoien et al. 2014](#)) and -14li ([Holoien et al. 2015](#)). The reported luminosities and total radiation energies above are respectively $L \simeq 8 \times 10^{43} \text{ erg s}^{-1}$ and $E_{\text{rad}} \simeq 2 \times 10^{50} \text{ erg}$ (former), $10^{44} \text{ erg s}^{-1}$ and $7 \times 10^{50} \text{ erg}$ (latter). We note that, if the SEDs of these two events are reddened by host-galaxy extinction, the true luminosities and energies are higher. Taking the reported L and E_{rad} as conservative values and assuming the pc-scale dust covering factor $f_\Omega = 0.1$, we expect the peak flux densities to be $\sim 0.03 \text{ mJy}$ for ASSASN-14ae

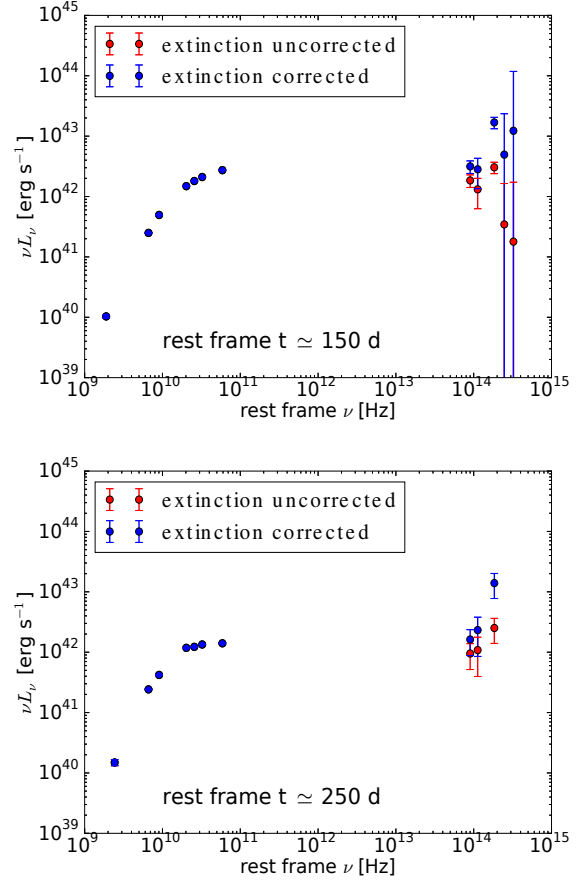


Figure 5. Spectral energy distributions of *Swift* J1644+57 at rest-frame time $t \simeq 150$ d (upper panel) and 250 d (lower panel). The radio data comes from [Zauderer et al. \(2013\)](#) and the radio flux from the host galaxy is negligible. The IR data comes from [Yoon et al. \(2015\)](#); [Levan et al. \(2015\)](#). The red points are host-subtracted fluxes. The blue points are further corrected for an extinction of $A_V = 10$ mag, following [Cardelli et al. \(1989\)](#) with $R_V = 3.1$.

and $\sim 0.5 \text{ mJy}$ for ASSASN-14li and peak wavelengths to be between 3 and $10 \mu\text{m}$ for both events.

To confirm the nature of dust IR emission, other possibilities can be ruled out in the following way: (1) unlike *Swift* J1644+57, the two ASSASN TDE candidates are not expected to have strong relativistic outflows and are hence radio quiet. Actually, [Alexander et al. \(2015\)](#) recently reported weak radio emission from ASSASN-14li, which was interpreted as a weak outflow driving an external shock. However, extrapolation from the radio to IR gives a flux much smaller than the predicted dust emission, so there is no contamination from the external shock. (2) With a good multi-wavelength coverage from mid-IR to optical, other components (such as the disk emission) could be separated out. (3) The contribution from the host galaxies could be subtracted by multi-epoch or high spacial resolution observations.

In future JWST mid-IR spectra, we can look for the smoking-gun evidences of dust, such as the silicate feature at $9.7 \mu\text{m}$ or polycyclic aromatic hydrocarbon (PAH) features.

4.2 Other observable signatures?

(1) If a significant amount of dust exists within $\sim 10^{18}$ cm, the refractory elements Al, Ca, Si and Fe, which normally condense into solids, will gradually return to the gas phase. Observing their abundances rising with time would be a direct evidence of dust sublimation. The abundances could be measured through absorption lines.

(2) If the dusty clouds lie along the line of sight, as dust grains sublime, the time evolution of dust extinction may be observable with sufficient UV and optical wavelength coverages.

(3) For simplicity, we have been assuming the source lightcurve to be flat, but TDEs actually have UV and optical variability down to at least timescales of days. Therefore, it may be possible to measure the time dependent dust IR emission in response to the variable UV and optical continuum. This so-called “dust reverberation mapping” method has been successfully used to determine the sublimation radius of the dusty torus in AGNs since the work by Clavel et al. (1989).

4.3 Some potential issues

In this subsection, we discuss some potential issues that may affect the details of the dust IR emission (but the general result in this work is unaffected).

(1) To solve the grain temperature, we have assumed instantaneous thermal equilibrium in eq.(4). This is valid because the heat capacity of a single grain is small, and hence the cooling time is short. Regardless of the composition, the upper limit of the total internal energy of a grain is $(\rho/\mu)(4\pi/3)a^3B \simeq 4 \times 10^{-3}a_{-5}^3$ erg. At a temperature of $T = 10^3T_3$ K, the radiative cooling rate is $\langle Q_{\text{abs}} \rangle_P 4\pi a^2 \sigma T^4 \simeq 3 \times 10^{-3}a_{-5}^2 T_3^5$ erg s $^{-1}$. Therefore, the cooling time is $< 1T_3^{-5}$ s, which means that dust grains reach thermal equilibrium nearly instantaneously.

(2) We have ignored dust destruction processes other than thermal sublimation. As mentioned by Waxman & Draine (2000) in the GRB context, photo-ionization of dust grains could lead to significant grain charging (positive). The electric field at the surface can be so large that the grain fragments (“Coulomb explosion”) or emits individual ions (“ion field emission”), depending on how strong the grain structure is. If the grain charge is $Z_g = 10^4 Z_{g,4}$ (in electron units), the electrostatic binding energy of an electron at the grain surface is $Z_g q^2/a \simeq 140 Z_{g,4} a_{-5}^{-1}$ eV (q being the electron charge). Photo-electric charging stops when the electrostatic binding energy exceeds the incoming photon’s energy. When exposed to the intense X-ray radiation from GRBs, the grain charge reaches $Z_g \simeq 10^5$ (Fruchter et al. 2001); but in the context of TDEs where the radiation energy is in UV and optical, the grain charge Z_g is smaller than 10^4 . The surface electric field is $Z_g q/a^2 = 1.4 \times 10^7 Z_{g,4} a_{-5}^{-2}$ V cm $^{-1}$, corresponding to a stress $S = E^2/4\pi \simeq 1.8 \times 10^8 Z_{g,4}^2 a_{-5}^{-4}$ dyne cm $^{-2}$. Ion field emission happens when the electric field approaches $\sim 10^8$ V cm $^{-1}$ (to break a typical 1 eV molecular bond across a distance of 1 Å). Coulomb explosion happens when the electrostatic stress is greater than the tensile strength of grains, which is uncertain. In the GRB literature (e.g. Fruchter et al. 2001), a typical grain tensile strength $S_{\text{max}} \simeq 10^{10}$ dyne cm $^{-2}$ is

used. Therefore, once the grain charge reaches $Z_g \simeq 10^5$, both Coulomb explosion and ion field emission can happen. However, neither of these two grain destruction mechanisms are important in the TDE context because the grain charge is too small. Even for relativistic TDEs like *Swift* J1644+57 with intense X-ray emission, since the X-rays are relativistically beamed into a narrow angle, most dusty clouds only receive the more-or-less isotropic UV-optical radiation.

(3) A few other complexities, which are ignored in our simple model, can be taken into account in future works. First, the heating by the scattered UV-optical photons and dust IR radiation could be included by considering the time delay and related absorption coefficient. In this way, a spectrum of dust IR emission can be calculated and compared with future observations. Second, the clumpiness of dusty clouds will affect the radiative transfer. Since every clump will have a bright (hot) side and a dark (cold) side, dust temperature distributions are different in clumpy and smooth environments. This is considered in modeling the IR emission from the AGN torus (Nenkova et al. 2008). Last, in the radiative transfer model in section 3, a single dust radius of $a = 0.1 \mu\text{m}$ is used, but the true interstellar grain population has a broad size distribution, extending from a few Å (PAH molecules) to about $0.2 \mu\text{m}$ (or even larger). Most mass is in the larger grains, with half-mass grain radius typically $\sim 0.1 \mu\text{m}$ (half of mass is in grains with radius above this value), and the smaller grains contribute most surface area and hence most UV extinction (e.g. Weingartner & Draine 2001; Laor & Draine 1993). However, at the same distance from the central source, smaller grains sublime faster than larger ones (mostly due to higher grain temperatures), so it is unclear which grain size contributes most IR emission. A systematic study of grain size distribution and chemical composition could be done in the future with dust continuum radiative transfer codes such as DUSTY⁸ and HYPERRION⁹, although the dynamical propagation of radiation coupled with dust sublimation requires some modification of the codes.

5 SUMMARY

We consider the impact of the UV-optical radiation ($E_{\text{rad}} \sim 10^{51} - 10^{52}$ erg) from TDEs on the circum-nuclear medium. If the medium is dusty, the UV-optical radiation energy will be absorbed by dust within ~ 1 pc from the BH and re-radiated in the IR. We calculate the bolometric lightcurve from a 1-D radiative transfer model, taking into account the time-dependent heating, cooling and sublimation of dust grains. We show that the dust emission peaks at $3 - 10 \mu\text{m}$ and has typical luminosities between 10^{42} and 10^{43} erg s $^{-1}$ (with sky covering factor f_{Ω} ranging from 0.1 to 1). This is detectable by current generation of telescopes, including the Stratospheric Observatory for Infrared Astronomy (SOFIA) and the *Spitzer* Space Telescope. In the near future, *James Webb* Space Telescope (JWST) will be able to perform photometric and spectroscopic measurements. In future JWST mid-IR spectra, we can look for the smoking-gun evidence of

⁸ <http://www.pa.uky.edu/~moshe/dusty/>

⁹ <http://www.hyperion-rt.org/>

dust, such as the silicate or polycyclic aromatic hydrocarbon (PAH) features.

Observations at rest-frame wavelength $\geq 2 \mu\text{m}$ have only been reported from two TDE candidates, SDSS J0952+2143 (Komossa et al. 2008, 2009) and *Swift* J1644+57 (Yoon et al. 2015; Levan et al. 2015). The *Spitzer* 10 – 20 μm flux of SDSS J0952+2143, although consistent with the dust emission from a TDE, is likely permanent emission from dusty starburst regions or an AGN. We also show that the *Spitzer* 3.6 μm and 4.5 μm fluxes of *Swift* J1644+57 may originate from other sources than the dust IR emission, such as the accretion disk or the external shock (driven by the interaction between disk outflow and circum-nuclear medium). Long-term monitoring is needed to tell whether the mid-IR emission from the two event is transient or permanent. Currently, a firm conclusion cannot be drawn. At last, we show that the two nearby TDE candidates ASSASN-14ae and -14li are good candidates to search for the dust IR emission. If the pc-scale dusty clouds have a sky covering factor of $f_{\Omega} = 0.1$, the conservatively estimated fluxes for the two events are, respectively, 0.03 mJy and 0.5 mJy at 3 – 10 μm .

AGNs are known to be surrounded by a dusty torus that provides obscuration and IR emission. However, little is known about the dust content in the pc-scale vicinity of weakly- or non-active galactic nuclei. Currently, the only observable example is our Galactic Center, where the dusty clouds has sky covering factor $f_{\Omega} \sim 30\%$ (Ferrière 2012). The dust IR emission can give a snapshot of the pc-scale dust content around weak- or non-active galactic nuclei, which is hard to probe otherwise.

6 ACKNOWLEDGMENTS

We acknowledge helpful discussions on the Galactic Center environment with J. Lacy. This research was funded by a graduate fellowship (named “Continuing Fellowship”) at the University of Texas at Austin. N.J.E. acknowledges support from a grant from the National Science Foundation, AST-1109116.

REFERENCES

- Alexander, K. D., Berger, E., Guillochon, J., Zauderer, B. A., & Williams, P. K. G. 2015, [arXiv:1510.01226](#)
- Arcavi, I., Gal-Yam, A., Sullivan, M., et al. 2014, *ApJ*, 793, 38
- Barniol Duran, R., & Piran, T. 2013, *ApJ*, 770, 146
- Bloom, J. S., Giannios, D., Metzger, B. D., et al. 2011, *Science*, 333, 203
- Cardelli, J. A., Clayton, G. C., & Mathis, J. S. 1989, *ApJ*, 345, 245
- Cenko, S. B., Krimm, H. A., Horesh, A., et al. 2012, *ApJ*, 753, 77
- Christopher, M. H., Scoville, N. Z., Stolovy, S. R., & Yun, M. S. 2005, *ApJ*, 622, 346
- Clavel, J., Wamsteker, W., & Glass, I. S. 1989, *ApJ*, 337, 236
- Draine, B. T., & Hao, L. 2002, *ApJ*, 569, 780
- Draine, B. T. 2011, *Physics of the Interstellar and Inter-galactic Medium* by Bruce T. Draine. Princeton University Press, 2011. ISBN: 978-0-691-12214-4,
- Elitzur, M., & Shlosman, I. 2006, *ApJL*, 648, L101
- Elitzur, M. 2008, *New Astronomy Reviews*, 52, 274
- Ferrière, K. 2012, *A&A*, 540, A50
- Fruchter, A., Krolik, J. H., & Rhoads, J. E. 2001, *ApJ*, 563, 597
- Gezari, S., Heckman, T., Cenko, S. B., et al. 2009, *ApJ*, 698, 1367
- Gezari, S., Chornock, R., Rest, A., et al. 2012, *Nature*, 485, 217
- González-Martín, O., Masegosa, J., Márquez, I., et al. 2015, *A&A*, 578, A74
- Guhathakurta, P., & Draine, B. T. 1989, *ApJ*, 345, 230
- Herrnstein, R. M., & Ho, P. T. P. 2005, *ApJ*, 620, 287
- Holoien, T. W.-S., Prieto, J. L., Bersier, D., et al. 2014, *MNRAS*, 445, 3263
- Holoien, T. W.-S., Kochanek, C. S., Prieto, J. L., et al. 2015, [arXiv:1507.01598](#)
- Jaffe, W., Meisenheimer, K., Röttgering, H. J. A., et al. 2004, *Nature*, 429, 47
- Jackson, J. M., Geis, N., Genzel, R., et al. 1993, *ApJ*, 402, 173
- Emmering, R. T., Blandford, R. D., & Shlosman, I. 1992, *ApJ*, 385, 460
- Komossa, S., Zhou, H., Wang, T., et al. 2008, *ApJL*, 678, L13
- Komossa, S., Zhou, H., Rau, A., et al. 2009, *ApJ*, 701, 105
- Komossa, S. 2015, *Journal of High Energy Astrophysics*, 7, 148
- Konigl, A., & Kartje, J. F. 1994, *ApJ*, 434, 446
- Krolik, J. H., & Begelman, M. C. 1988, *ApJ*, 329, 702
- Kumar, P., Barniol Duran, R., Bošnjak, Ž., & Piran, T. 2013, *MNRAS*, 434, 3078
- Kumar, P., & Zhang, B. 2015, *Physics Reports*, 561, 1
- Lacy, J. H., Townes, C. H., & Hollenbach, D. J. 1982, *ApJ*, 262, 120
- Laor, A., & Draine, B. T. 1993, *ApJ*, 402, 441
- Lau, R. M., Herter, T. L., Morris, M. R., Becklin, E. E., & Adams, J. D. 2013, *ApJ*, 775, 37
- Lau, R. M., Herter, T. L., Morris, M. R., Li, Z., & Adams, J. D. 2015, *Science*, 348, 413
- Levan, A. J., Tanvir, N. R., Cenko, S. B., et al. 2011, *Science*, 333, 199
- Levan, A. J., Tanvir, N. R., Brown, G. C., et al. 2015, [arXiv:1509.08945](#)
- Loeb, A., & Ulmer, A. 1997, *ApJ*, 489, 573
- Lu, W., Kumar, P. 2015, submitted to *MNRAS*
- Metzger, B. D., Giannios, D., & Mimica, P. 2012, *MNRAS*, 420, 3528
- Metzger, B. D., & Stone, N. C. 2015, [arXiv:1506.03453](#)
- Miller, M. C. 2015, *ApJ*, 805, 83
- Mimica, P., Giannios, D., Metzger, B. D., & Aloy, M. A. 2015, *MNRAS*, 450, 2824
- Nenkova, M., Sirocky, M. M., Nikutta, R., Ivezić, Ž., & Elitzur, M. 2008, *ApJ*, 685, 160
- Netzer, H., Lutz, D., Schweitzer, M., et al. 2007, *ApJ*, 666, 806
- Piran, T., Svirski, G., Krolik, J., Cheng, R. M., & Shiohara, H. 2015, *ApJ*, 806, 164
- Rees, M. J. 1988, *Nature*, 333, 523

- Roberts, D. A., & Goss, W. M. 1993, *ApJS*, 86, 133
- Scoville, N. Z., Stolovy, S. R., Rieke, M., Christopher, M., & Yusef-Zadeh, F. 2003, *ApJ*, 594, 294
- Serabyn, E., & Lacy, J. H. 1985, *ApJ*, 293, 445
- Shakura, N. I., & Sunyaev, R. A. 1973, *A&A*, 24, 337
- Strubbe, L. E., & Quataert, E. 2009, *MNRAS*, 400, 2070
- Tristram, K. R. W., Meisenheimer, K., Jaffe, W., et al. 2007, *A&A*, 474, 837
- Ulmer, A. 1999, *ApJ*, 514, 180
- van Velzen, S., Farrar, G. R., Gezari, S., et al. 2011, *ApJ*, 741, 73
- Vinkó, J., Yuan, F., Quimby, R. M., et al. 2015, *ApJ*, 798, 12
- Wang, J., & Merritt, D. 2004, *ApJ*, 600, 149
- Waxman, E., & Draine, B. T. 2000, *ApJ*, 537, 796
- Weingartner, J. C., & Draine, B. T. 2001, *ApJ*, 548, 296
- Yoon, Y., Im, M., Jeon, Y., et al. 2015, *ApJ*, 808, 96
- Zauderer, B. A., Berger, E., Soderberg, A. M., et al. 2011, *Nature*, 476, 425
- Zauderer, B. A., Berger, E., Margutti, R., et al. 2013, *ApJ*, 767, 152